

ChemComm

Accepted Manuscript



This is an *Accepted Manuscript*, which has been through the Royal Society of Chemistry peer review process and has been accepted for publication.

Accepted Manuscripts are published online shortly after acceptance, before technical editing, formatting and proof reading. Using this free service, authors can make their results available to the community, in citable form, before we publish the edited article. We will replace this *Accepted Manuscript* with the edited and formatted *Advance Article* as soon as it is available.

You can find more information about *Accepted Manuscripts* in the [Information for Authors](#).

Please note that technical editing may introduce minor changes to the text and/or graphics, which may alter content. The journal's standard [Terms & Conditions](#) and the [Ethical guidelines](#) still apply. In no event shall the Royal Society of Chemistry be held responsible for any errors or omissions in this *Accepted Manuscript* or any consequences arising from the use of any information it contains.

COMMUNICATION

Polyimide-wrapped carbon nanotube electrodes for long cycle Li-air batteries

Cite this: DOI:
10.1039/x0xx00000x

Chan Kyu Lee^a and Yong Joon Park^{a*}

Received 00th January 2012,
Accepted 00th January 2012

DOI: 10.1039/x0xx00000x

www.rsc.org/

A simple surface modification technique for carbon electrodes in long-cycle Li-air batteries is demonstrated, in which a polyimide coating is used to suppress unwanted side reactions between the electrode and electrolyte (and/or Li_2O_2). This is found to result in excellent cyclic performance, without any significant loss of capacity.

Rechargeable Li-air batteries are currently the subject of much attention due to the expectation that they can allow energy densities to be achieved that are several times greater than even the most state-of-the-art lithium-ion batteries.¹ However, there are still a number of fundamental and practical challenges that need to be overcome with regards to their low rate capability, limited cycle life and significant overpotential.² These stem from the fact that the electrochemistry of a non-aqueous Li-air cell is based on the formation and dissociation of solid reaction products such as Li_2O_2 , and since this reversible reaction occurs on the surface of the electrode, the properties of the cell are largely determined by the nature of the electrode. Carbon has tended to be the base material of choice for electrodes because of its high conductivity, low weight and wide surface area; and when used as an air electrode, can provide redox reaction sites and a large area for the storage of reaction products.² However, recent studies have confirmed that carbon is unfortunately also a primary cause of unwanted side reactions.³ For example, in the presence of Li_2O_2 produced by the discharge process, carbon can easily react with Li_2O_2 and undergo oxidative decomposition to Li_2CO_3 at high voltage. Furthermore, the surface of carbon promotes electrolyte decomposition during discharging and charging cycles, giving rise to organic material such as Li carboxylates.³ Since neither the Li_2CO_3 nor organic material is easily dissociated on charging, they tend to accumulate with successive cycles and therefore lead to a high overpotential and limited cyclic performance in Li-air cells.⁴

A possible solution to the problems associated with carbon electrodes in Li-air batteries is of course to design a suitable carbon-free electrode. Indeed, several groups have already made progress in

this regard using inorganic materials such as Co_3O_4 and TiC ,⁵ and have demonstrated an improved cyclic performance as a result.

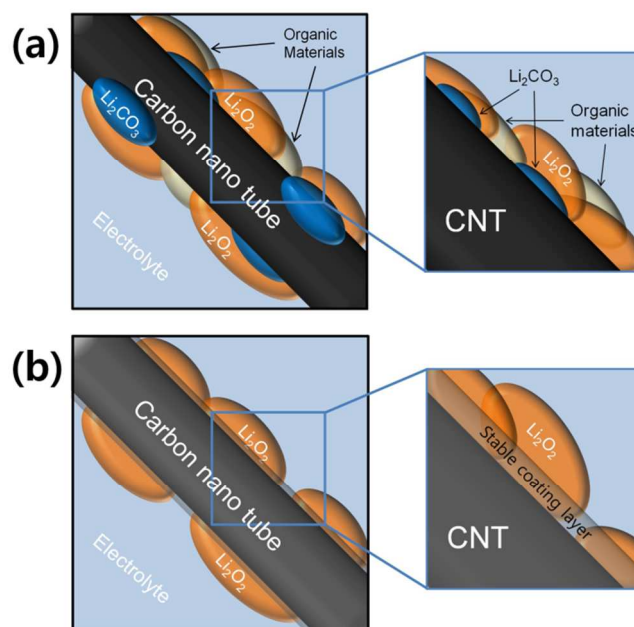


Figure 1 Schematic diagram showing the reaction between a carbon-based electrode and electrolyte (and/or Li_2O_2) for: (a) an electrode employing pristine carbon, and (b) an electrode employing surface-modified carbon.

However, this comes at expense of significantly lower capacity compared to carbon-based electrodes due to the high weight of inorganic electrode materials. Therefore, in this study, we propose using a stable surface coating on a carbon electrode as a new approach to reducing the instability of carbon-based air electrodes. The schematic in Figure 1 shows the difference in structure between

a surface-coated electrode and a conventional carbon-based electrode. As shown in Fig. 1a, the side reaction between carbon and the electrolyte (and/or Li_2O_2) results in unwanted reaction products that reduce electrochemical performance. In contrast, the stable coating shown in Fig. 1b limits direct contact between the carbon and electrolyte (and/or Li_2O_2), thereby suppressing the formation of unwanted reaction products. Moreover, given that the bulk of the electrode is still, it should be possible to achieve a much higher capacity than a carbon-free electrode.

The stable coating material used in this study was a polyimide coating layer prepared through the imidization of a polyamic acid solution. This produced a highly continuous surface coverage with a nanometer thickness, and can provide both chemical and thermal stability.⁶ Indeed, polyimide coatings have already been applied to the cathode materials of lithium ion batteries to prevent them reacting with the electrolyte, and so it stands to reason that a polyimide coating should also prevent the unwanted side reaction between a carbon air electrode and electrolyte (and/or Li_2O_2). For the carbon electrode, carbon nanotubes (CNTs) were chosen as these have been successfully used for air electrodes in Li-air cells.⁷

The TEM images of the pristine and polyimide coated CNTs in Figure 2 show that although the pristine CNTs have the smooth side walls characteristic of multi-walled CNTs, the polyimide-coated CNTs are covered with a film-type shell of polyimide, which has a lighter contrast than the side walls of the pristine CNTs. The composition of the surface of both the pristine and polyimide coated CNTs (highlighted by the red rectangles in Fig. 2e and 2f) was investigated by energy-dispersive X-ray spectroscopy (EDS). As evident from the insets in Fig. 2e and 2f, the polyimide-coated CNT surfaces have a relatively higher N content than the surface of a pristine CNT, which confirms the presence of the coating layer. EDS mapping was also used to verify the uniformity of the coating layer, with the red square in Fig. 1g showing the area that was analyzed, and Fig. 2h and 2i showing the resulting EDS maps for C and N. This reveals that both C and N are uniformly distributed over the area in question, indicating a homogenous attachment of the coating to the surface of the CNT. The FTIR peaks of the polyimide-coated CNT further confirm that the coating layer is polyimide, as shown in Fig. 3a, with the broad peaks between 1710 – 1770 cm^{-1} being associated with the C=O bond of polyimide.⁶

To characterize the effects of the polyimide coating, the electrochemical performance of air electrodes employing pristine and polyimide-coated CNTs were observed and compared. For convenience, the electrode employing polyimide-coated CNTs is hereafter referred to as the “PI electrode,” and the electrode employing untreated CNTs as the “pristine electrode.” Figure 3b shows the initial discharge-charge profiles of both electrodes at a current density of $500\text{ mA}\cdot\text{g}^{-1}$ within a voltage range of 2.35 – 4.35 V . The capacity was determined based on the total electrode mass (CNT+binder), and as shown in Fig. 3b, the PI electrode exhibited a slightly lower discharge capacity than the pristine electrode. This is most likely attributable to the low conductivity of the polyimide layer and/or a decrease in the surface area of the carbon. The overpotential appears to increase slightly due to the polyimide layer, but this is of minimal importance to the overall performance. The surface resistance of the pristine electrode was $\sim 19\ \Omega/\text{sq}$ compared with $\sim 23\ \Omega/\text{sq}$ for the PI electrode, which indicates that the thin polyimide layer does not significantly reduce the conductivity of the electrode. What is important, however, is whether the surface coating affects the formation of reaction products. To check this, XRD patterns of the pristine and PI electrode were acquired before

and after the initial (full) discharge of the cell (Fig. 3c). Note that with both electrodes there is clear evidence that Li_2O_2 was formed, thus indicating that the polyimide layer does not disturb the formation of Li_2O_2 .

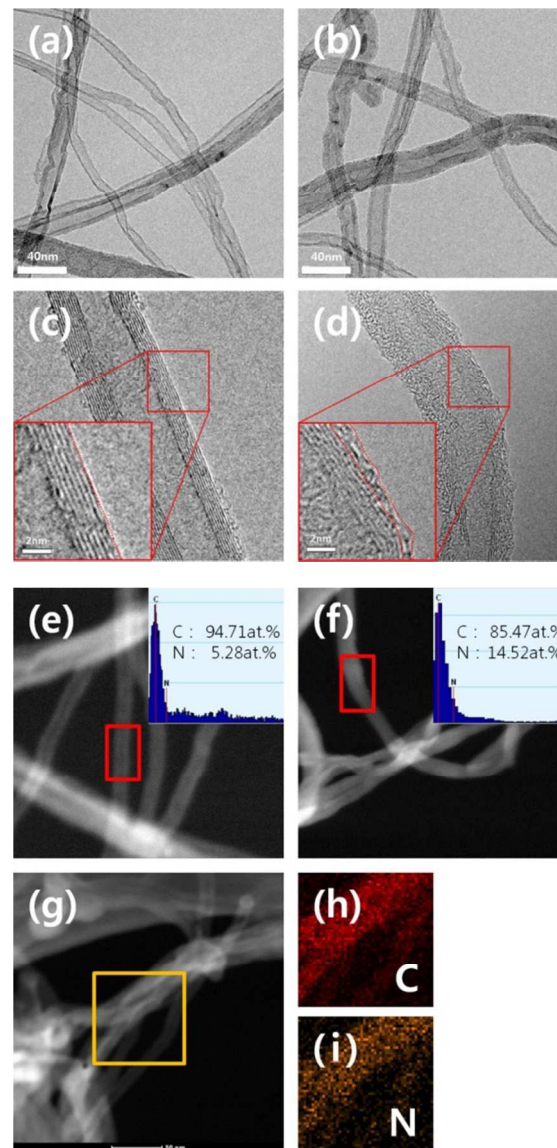


Figure 2 (a, c) TEM images of pristine CNTs; (b, d) TEM images of polyimide-coated CNTs; (e) EDS results for pristine CNTs; (f) EDS results for polyimide-coated CNTs; (g) TEM image of polyimide-coated CNTs showing the area analyzed by EDS mapping (denoted by the yellow square); (h) EDS map of C; (i) EDS map of N.

The cyclic performance of the pristine and PI electrodes at a current density of $500\text{ mA}\cdot\text{g}^{-1}$ are presented in Fig. 3d, with the cells being cycled at a limited capacity of $1500\text{ mAh}\cdot\text{g}_{\text{electrode}}^{-1}$ in order to prevent a large depth-of-discharge.⁸ The voltage range was 2.0 – 4.35 V , and the upper potential (4.35 V) was held until the current density reached $2\text{ mA}\cdot\text{g}^{-1}$ during charging in order to facilitate the decomposition of reaction products. It can be seen from this that the pristine electrode maintained its capacity for 65 cycles, which is likely due to the accumulated reaction products (most of those are

expected as unwanted reaction products) disturbing the reaction between Li ions and oxygen in the electrode. Whereas the PI electrode had a greatly enhanced cyclic performance in that it was able to maintain its capacity for 137 cycles. This confirms that a polyimide coating can play a vital role in improving the cyclic performance of carbon-based electrodes for Li-air cells.

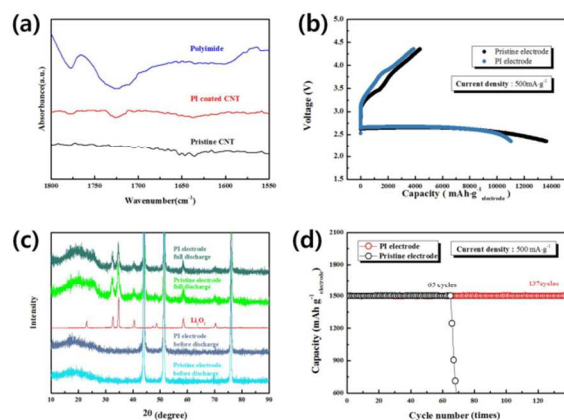


Figure 3 (a) FTIR spectrum of pristine and PI-coated CNTs; (b) initial discharge-charge profiles of both electrodes; (c) XRD patterns of both electrodes before testing and after the initial (full) discharge; (d) cyclic performance of the electrodes at $1500 \text{ mAh} \cdot \text{g}^{-1}$.

Also of note is the fact that the capacity of this cycling test ($1500 \text{ mAh} \cdot \text{g}_{\text{electrode}}^{-1}$) was much higher than that of a typical carbon-free electrode (usually less than $500 \text{ mAh} \cdot \text{g}_{\text{electrode}}^{-1}$).⁵ The discharge-charge profiles in Figure S1 (see supplementary information) also revealed that the charge-voltage of the pristine electrode increases more rapidly than that of the PI electrode, further confirming the superior cyclic performance of the PI electrode.

As mentioned earlier, the cyclic performance of a non-aqueous Li-air cell is highly affected by unwanted side reactions such as the formation of Li_2CO_3 and decomposition of the electrolyte.^{3,4} Given this, the enhanced cyclic performance of the PI electrode could easily be explained by the polyimide layer preventing direct contact between the electrode and the electrolyte and/or Li_2O_2 . To confirm this SEM images were obtained for the pristine and PI electrodes, which as shown in Fig. 4c and 4d, revealed the surface of both electrodes to be covered with reaction products after the initial discharge. Most of these products were subsequently dissociated after initial charging, but as shown in Fig. 4e and 4f, some reaction products appear to have remained. The morphology of both electrodes during this initial cycle was essentially identical, but a very pronounced difference became apparent after 50 cycles. As shown in Fig. 4g, most of the CNT fibers of the pristine electrode became fully buried under reaction products, even when in a charged state, which implies that its access to the electrolyte would be seriously impeded. In contrast, the polyimide coating resulted in far less accumulation of reaction products, with the surface of the PI electrode after 50 cycles still clearly exhibiting fiber-like shapes, vacant space and numerous holes allowing easy access to the electrolyte. This reduction of accumulated reaction products is therefore considered a major factor in the enhanced cyclic performance of the PI electrode.

To investigate the nature of the reaction products in greater detail, FTIR spectra were collected from the pristine and PI electrode after

50 cycles (charged state). As shown in Fig. 5 the spectra of the pristine electrode exhibited peaks at $400\text{-}500$, $600\text{-}700$, $1350\text{-}1500$, and $1500\text{-}1700 \text{ cm}^{-1}$ (marked with ★) that are considered to be the result of organic materials such as $\text{CH}_3\text{CO}_2\text{Li}$ and HCO_2Li created by side reactions with the electrolyte (note that HCO_2Li has a similar FTIR spectrum to $\text{CH}_3\text{CO}_2\text{Li}$). Meanwhile, the broad peak between $1400\text{-}1500$ and sharp peak at $\sim 500 \text{ cm}^{-1}$ are attributed to Li_2CO_3 , but this is very difficult to identify given its similarity to the FTIR spectrum of Li_2O_2 that has been exposed to air.

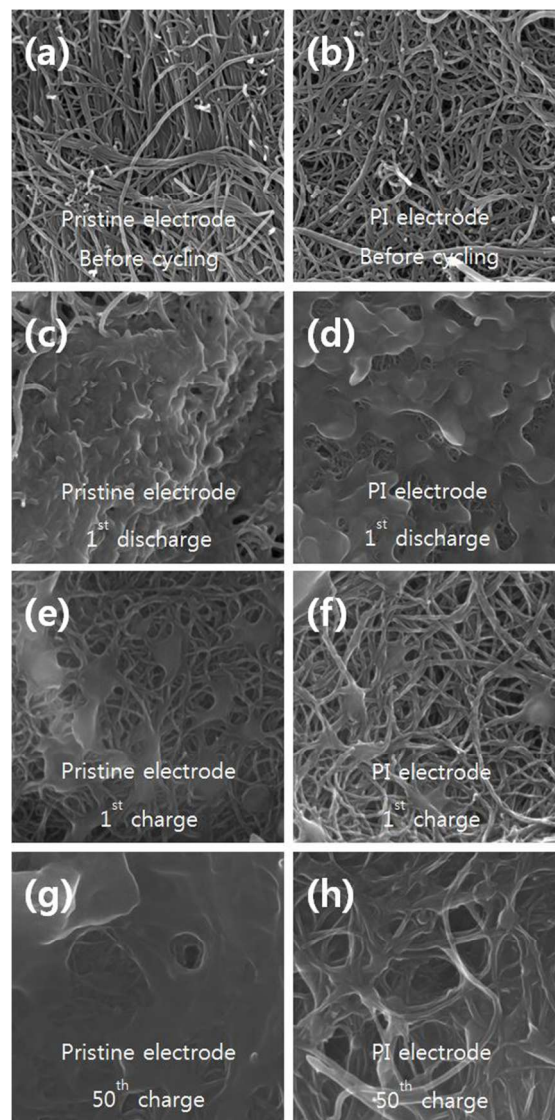


Figure 4 SEM images of: (a) a pristine electrode before cycling; (b) a PI electrode before cycling; (c) a pristine electrode after initial discharge; (d) a PI electrode after initial discharge; (e) a pristine electrode after initial charge; (f) a PI electrode after initial charge; (g) a pristine electrode after its 50th charge; (h) a PI electrode after its 50th charge.

To make matter worse, some of the Li_2CO_3 peaks overlap with the peaks of the organic material. Nevertheless, it is clear that there is a greater accumulation of reaction products associated with unwanted side reactions on the pristine electrode after 50 cycles, as evidenced by the lower intensity of the relevant peaks in the spectrum of the PI electrode (see Figure S2 in the supplementary information for a

magnified view of Fig. 5a). This further confirms the effectiveness of the polyimide coating, in that although the side reactions still occur, their impact on the cyclic performance is greatly reduced. Nyquist plots of cells employing pristine and PI electrodes before test and after 50 cycles (charged state) can be found in Fig. S3 (see supplementary information), and these indicate that although there is no difference in impedance prior to testing, the impedance of the cell with a PI electrode is lower after 50 cycles.

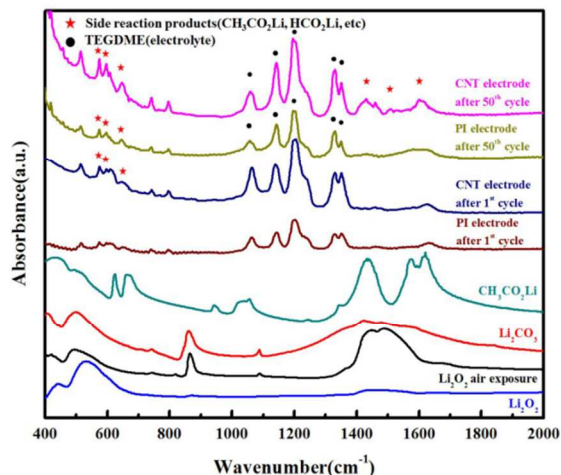


Figure 5 FTIR spectra of pristine and PI-coated electrodes after 1 and 50 cycles (charged state)

Conclusions

The application of a polyimide coating to CNTs used in the fabrication of an electrode materials for long-cycle Li-air batteries has been shown to effectively suppress unwanted side reactions between the electrode and electrolyte (and/or Li_2O_2) by preventing their direct contact. The reduced buildup of reaction products that results from this is considered the main reason for the greatly enhanced cyclic performance that was observed in the case of a Li-air cell based on a polyimide-coated electrode at a capacity much greater than can be achieved with current carbon-free electrode technologies.

“This research was supported by Basic Science Research Program through the National Research Foundation of Korea (NRF) funded by the Ministry of Science, ICT and future Planning (No.2014R1A2A2A01003542) and by the Energy Efficiency & Resources Core Technology Program of the Korea Institute of Energy Technology Evaluation and Planning (KETEP), granted financial resource from the Ministry of Trade, Industry & Energy, Republic of Korea. (No. 20112020100110/KIER B4-2462)”. “This work was also supported by the National Research Foundation of Korea Grant funded by the Korean Government (MEST) (NRF-2009-0094232)”.

Notes and references

^a Department of Advanced Materials Engineering, Kyonggi University, 154-42 Gwanggyosan-ro, Yeongtong-gu, Suwon-si, Gyeonggi-Do, 443-760, Korea

* yjpark2006@kyonggi.ac.kr

Electronic Supplementary Information (ESI) available: See

DOI: 10.1039/c000000x/

1. F. Li, H. Kitaura and H. Zhou, *Energy Environ. Sci.*, 2013, **6**, 2302; F. Li, T. Zhang and H. Zhou, *Energy Environ. Sci.*, 2013, **6**, 1125; D. Zhu, L. Zhang, M. Song, X. Wang and Y. Chen, *Chem. Commun.*, 2013, **49**, 9573; G. Zhao, Z. Xu and K. Sun, *J. Mater. Chem. A*, 2013, **1**, 12862; H. Kim, H.-D. Lim, J. Kim and K. Kang, *J. Mater. Chem. A*, 2014, **2**, 33.
2. R. Black, B. Adams and L. F. Nazar, *Adv. Energy Mater.*, 2012, **2**, 801; F. Li, T. Zhang and H. Zhou, *Energy Environ. Sci.*, 2013, **6**, 1125; T. H. Yoon and Y. J. Park, *J. Power Sources*, 2013, **244**, 344; A. Kraytsberg and Y. Ein-Eli, *J. Power Sources*, 2011, **196**, 886; R. Padbury and X. Zhang, *J. Power Sources*, 2011, **196**, 4436; J. Christensen, P. Albertus, R. S. Sanchez-Carrera, T. Lohmann, B. Kozinsky, R. Liedtke, J. Ahmed and A. Kojic, *J. Electrochem. Soc.*, 2012, **159**, R1; C. S. Park, K. S. Kim and Y. J. Park, *J. Power Sources*, 2013, **244**, 72; W.-H. Ryu, T. H. Yoon, S. H. Song, S. Jeon, Y. J. Park and I. D. Kim, *Nano Lett.*, 2013, **9**, 4190. F. Cheng, J. Chen, *Chem. Soc. Rev.*, 2012, **41**, 2172.
3. M. M. O. Thotiyl, S. A. Freunberger, Z. Peng and P. G. Bruce, *J. Am. Chem. Soc.*, 2013, **135**, 494; B. D. McCloskey, A. Speidel, R. Scheffler, D. C. Miller, V. Viswanathan, J. S. Hummelshøj, J. K. Nørskov and A. C. Luntz, *J. Phys. Chem. Lett.*, 2012, **3**, 997; J. Lu, Y. Lei, K. C. Lau, X. Luo, P. Du, J. Wen, R. S. Assary, U. Das, D. J. Miller, J. W. Elam, H. M. Albishri, D. A. El-hady, Y. K. Sun, L. A. Curtiss and K. Amine, *Nat. Commun.*, 2013, **4**, 2383.
4. Y.-C. Lu and Y. Shao-Horn, *J. Phys. Chem. Lett.*, 2013, **4**, 93; B. M. Gallant, R. R. Mitchell, D. G. Kwabi, J. Zhou, L. Zuin, C. V. Thompson and Y. Shao-Horn, *J. Phys. Chem. C*, 2012, **116**, 20800.
5. M. O. Thotiyl, S. A. Freunberger, Z. Peng, Y. Chen, Z. Liu and P. G. Bruce, *Nature Mater.*, 2013, **12**, 1050; A. Riaz, K.-N. Jung, W. Chang, S.-B. Lee, T.-H. Lim, S.-J. Park, R.-H. Song, S. Yoon, K.-H. Shin and J.-W. Lee, *Chem. Commun.*, 2013, **49**, 5984; Y. Cui, Z. Wen and Y. Liu, *Energy Environ. Sci.*, 2011, **4**, 4727.
6. J.-H. Cho, J.-H. Park, M.-H. Lee, H.-K. Song and S.-Y. Lee, *Energy Environ. Sci.*, 2012, **5**, 7124; J.-H. Park, J.-S. Kim, E.-G. Shim, K.-W. Park, Y. T. Hong, Y.-S. Lee and S.-Y. Lee, *Electrochem. Commun.*, 2010, **12**, 1099–1102.
7. T. H. Yoon and Y. J. Park, *RSC Adv.*, 2014, **4**, 17434; D. S. Kim and Y. J. Park, *Electrochimica Acta*, 2014, **132**, 297–306.
8. A. Débart, A. J. Paterson, J. Bao and P.G. Bruce, *Angew. Chem.*, 2008, **47**, 4521; D. S. Kim, Y. J. Park, *J. Alloys Comp.*, 2014, **591**, 164–169.

